Cross sections for elastic electron scattering by tetramethylsilane in the intermediate-energy range

R. T. Sugohara,[1] M.-T. Lee,[2] G. L. C. de Souza,[3] M. G. P. Homem,[4] and I. Iga[2]
[1]*Departamento de Física, UFSCar, 13565-905 São Carlos, SP, Brazil*
[2]*Departamento de Química, UFSCar, 13565-905 São Carlos, SP, Brazil*
[3]*Instituto de Ciências Exatas e Tecnologia, UFAM, 69100-000 Itacoatiara, AM, Brazil*
[4]*Departamento de Física, UFSC, 88010-970 Florianópolis, SC, Brazil*
(Received 27 October 2011; published 9 December 2011)

Organosilicon compounds are of current interest due to the numerous applications of these species in industries. Some of these applications require the knowledge of electron collision cross sections, which are scarce for such compounds. In this work, we report absolute values of differential, integral, and momentum-transfer cross sections for elastic electron scattering by tetramethylsilane (TMS) measured in the 100–1000 eV energy range. The relative-flow technique is used to normalize our data. In addition, the independent-atom-model (IAM) and the additivity rule (AR), widely used to model electron collisions with light hydrocarbons, are also applied for e^--TMS interaction. The comparison of our measured results of cross sections and the calculated data shows good agreement, particularly near the higher-end of incident energies.

DOI: 10.1103/PhysRevA.84.062709 PACS number(s): 34.80.Bm

I. INTRODUCTION

Silicon-organic compounds are widely used in many technological applications. For instance, organosilyl halides are extensively used as reagents in organic chemistry [1]. Organosilicons are also important in the semiconductor industries because they contain silicon atom. They are applied in plasma polymerization and in plasma-assisted deposition processes [2–4] as well. Further, mixtures of tetramethylsilane (TMS) and argon are used for silicon carbide coatings by plasma-assisted chemical vapor-deposition processes [5,6].

For the latter application, the understanding of the chemistry of TMS in plasma environment is very important. Modeling of TMS plasmas requires fundamental data like electron transport parameters in both pure TMS and its mixtures and also accurate knowledge of a variety of electron collision cross sections in function of incident energy. Unfortunately, for this target of interest, absolute values of electron-collision cross sections are, in general, scarce. Only limited experimental studies were reported in the literature over the years. For instance, absolute partial (PICS) and total (TICS) ionization cross sections for electron-TMS impact were reported by McGinnis *et al.* [7] in the 30–70 eV energy range and lately also by Basner *et al.* [3] at incident energies from the threshold to 90 eV. Electron-impact vibrational excitation function and also excitation function of some electronic transitions of TMS were measured by Huber *et al.* [8] in the 0–11 eV incident energy range. More recently, absolute values of elastic momentum-transfer cross sections (MTCS), vibrational and electronic excitation cross sections, as well as TICS and attachment cross sections were determined by Bordage *et al.* [4], using the swarm analysis technique based on the solution of Boltzmann equation. Nevertheless, to our knowledge, there is no other type of cross sections, e.g., elastic differential (DCS) and integral (ICS) cross sections for electron-TMS collision, ever measured and reported. In this sense, a systematic experimental study of electron interaction with TMS is clearly of interest not only to supply more data for technological applications, but it also constitutes a model for larger organosilicon systems since TMS is the simplest member of this series.

From a theoretical point of view, there is also a lack of cross-section calculations for elastic electron-TMS collisions in the literature. To present, the few theoretical results for electron-TMS collision refer to the TICS calculated using the modified-additivity-rule (MAR) [13] and those with the binary-encounter theory and the dipole interaction of the Bethe theory (BEB) model [14]. It is known that at incident energies above the ionization threshold, the influence of inelastic scattering channels, including both the excitation and ionization processes, on the elastic channel is important. The competition between the elastic and inelastic scattering processes leads to a reduction of the flux of elastically scattered electrons. Although some recently developed theoretical methods were successfully applied to calculate elastic and total cross sections (TCS) for electron scattering by some small molecules [15–17], the extension of their application to larger targets is still under investigation. On the other hand, the independent-atom-model (IAM) and additivity rule (AR) have shown to be effective to treat e^--molecule interaction in the energy range of hundreds of eV. However, their application is mostly focused at targets constructed by light atoms such as hydrogen, carbon, nitrogen, and oxygen [18,19]. The validity of such methods for targets that contain heavier atoms is still to be tested.

In this work we present an experimental investigation on elastic scattering of electrons by TMS in the intermediate energy range. Particularly, DCS, ICS, and MTCS in the 100–1000 eV energy range are reported. The present work constitutes an attempt to partially fill the above-mentioned lack of data. These physical quantities are also calculated in the present work using the IAM and AR. A complex optical potential (COP) composed of the static, exchange, polarization, and absorption contributions is used to represent the electron-atom interaction. Comparison of the calculated results with our experimental data may provide insights of the application of IAM and AR to other silicon-containing systems.

The organization of this paper is as follows: In Sec. II, we present our experimental procedures. In Sec. III, some

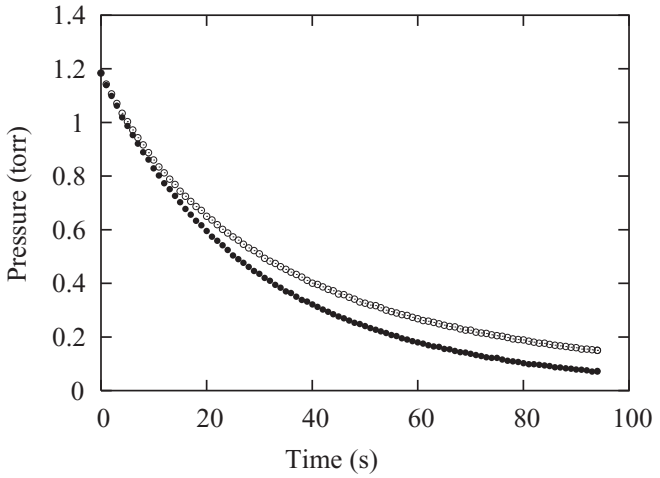

FIG. 1. *P-t* curves for TMS (solid circles) and benzene (open circles), at 25 °C.

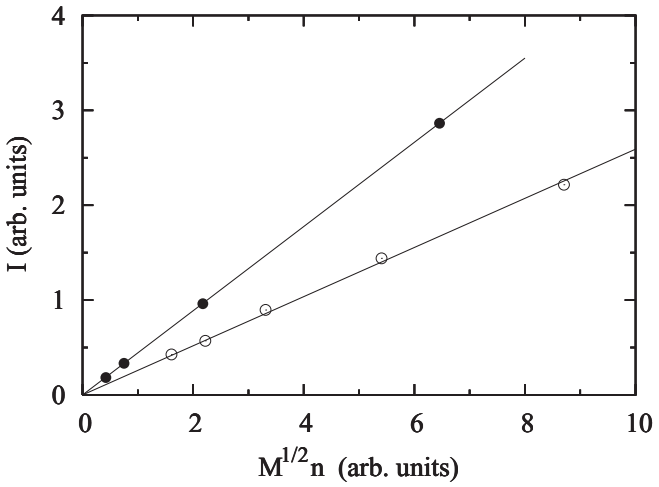

FIG. 2. Intensity of the scattered electron versus relative flow-rate $M^{1/2}R$ taken at 100 eV and 25°. Solid circles, experimental data for TMS; open circles, data for Ar; solid lines, the fitted results.

details of the calculations are briefly described as well. Finally, in Sec. IV, our measured results are compared with the present calculated results using the IAM at the static-exchange-polarization-absorption (SEPA) level of approximation. Some conclusive remarks are presented in Sec. V.

II. EXPERIMENT

Details of our experimental setup and procedure have already been presented in previous works [20,21] and will only be briefly described here. At a given incident electron energy, relative angular distributions of the energy-filtered electrons with an overall resolution of about 1.5 eV, scattered elastically by TMS, are measured using an electron beam–molecular beam geometry. Therefore, inelastically scattered electrons resulted from electronic excitation and ionization processes are discriminated, since the lowest excitation threshold of TMS is 7.45 eV [8]. Nevertheless, it is unable to separate those from vibrational excitation processes.

The measured relative angular distributions are converted to absolute DCS using the relative-flow technique (RFT) [9,10], according to

$$\left(\frac{d\sigma}{d\Omega}\right)_x = \left(\frac{d\sigma}{d\Omega}\right)_{\text{std}} \frac{I_x}{I_{\text{std}}} \frac{R_{\text{std}}}{R_x} \left(\frac{M_{\text{std}}}{M_x}\right)^{\frac{1}{2}}, \quad (1)$$

where I is the intensity of electrons measured at a given scattering angle, R is the relative-flow rate, and M is the molecular weight. The subindices x and std refer to the gas

TABLE I. Experimental DCS (in Å^2/sr), ICS and MTCS (in Å^2) for elastic e^--TMS scattering. The notation 1.25[2] denotes 1.25×10^2.

Angle (deg)	E_0 (eV)					
	100	200	300	400	500	1000
5	1.25[2]	6.63[1]	7.20[1]		2.51[1]	
8	3.83[2]	1.40[1]	2.30[1]	1.59[1]		1.05[1]
10	3.25[1]	1.18[1]	7.73[0]	9.80[0]	9.04[0]	6.78[0]
15	5.59[0]	6.16[0]	5.94[0]	5.58[0]	4.22[0]	3.01[0]
20	3.89[0]	3.65[0]	2.33[0]	2.51[0]	2.89[0]	9.64[−1]
25	2.89[0]	1.53[0]	1.77[0]	1.91[−1]	1.27[0]	6.10[−1]
30	1.48[0]	1.30[0]	1.31[0]	7.51[−1]	7.19[−1]	3.44[−1]
40	6.61[−1]	6.00[−1]	4.35[−1]	4.17[−1]	3.08[−1]	1.38[−1]
50	5.69[−1]	3.03[−1]	2.22[−1]	2.01[−1]	1.58[−1]	6.70[−2]
60	2.56[−1]	2.25[−1]	1.69[−1]	1.25[−2]	9.79[−2]	3.45[−2]
70	1.59[−1]	1.43[−1]	9.98[−2]	8.10[−2]	6.00[−2]	2.19[−2]
80	1.65[−1]	1.15[−1]	7.70[−2]	5.59[−2]	4.23[−2]	1.61[−2]
90	1.30[−1]	9.35[−2]	6.27[−2]	5.26[−2]	3.50[−2]	1.38[−2]
100	1.23[−1]	7.84[−2]	4.78[−2]	3.92[−2]	2.90[−2]	1.14[−2]
110	1.23[−1]	6.73[−2]	5.27[−2]	4.66[−2]	2.85[−2]	9.97[−3]
120	1.59[−1]	7.71[−2]	5.90[−2]	3.82[−2]	2.64[−2]	1.01[−2]
130	2.01[−1]	9.38[−2]	7.38[−2]	4.89[−2]	2.73[−2]	9.10[−3]
ICS	1.80[1]	1.02[1]	8.20[0]	5.67[0]	4.77[0]	2.90[0]
MTCS	2.92[0]	1.64[0]	1.22[0]	9.00[−1]	6.54[−1]	2.55[−1]

under determination and the secondary standard, respectively. The application of RFT requires the precise measurement of R for both x and std. Since TMS is liquid at room temperature, its vapor when injected into the scattering chamber may be adsorbed on the inner surfaces, which may lead to errors in relative-flow-rate determination and, consequently, also in the absolute calibration of DCS. In order to avoid such errors, we have recently developed a systematic procedure [11] for accurate relative-flow-rate determination of gases and vapors. The method reported in that study has already been applied to evaluate the influence of the adsorption effects in the CS determination of methanol [12] and is also applied here.

During the measurements, the working pressure in the vacuum chamber is around 5×10^{-7} torr. TMS in gas phase was obtained from the saturated vapor above a liquid sample in a vail attached to a metallic gas manifold. The liquid sample underwent several freeze-thaw cycles in order to eliminate possible contaminants, mostly atmospheric air. During the measurements, the liquid sample was maintained at 0 °C, whereas the gas manifold was at room temperature.

In the present study, the R of both the target under study and the secondary standard (Ar) were determined using the method of pressure decrease (MPD) according to the procedure presented elsewhere [11]. Using this method, the R is simply given by

$$R = -\left(\frac{dP}{dt}\right)_{P=P_s}, \tag{2}$$

where P_s is the steady pressure inside of the reservoir when the scattering measurements are carried out. As an example, in Fig. 1, we present experimental P-t curves of TMS and benzene obtained at room temperature (25 °C). It is interesting to note a significant difference between the experimental pressure-decrease curves of TMS and benzene. Despite benzene being lighter than TMS, its pressure decrease with time is substantially slower than that of TMS, indicating that the adsorption of benzene on the surfaces is relevant. In fact, the desorption of benzene molecules from surfaces could contribute to this slower drop of pressure. Also, our study revealed that the effect of adsorption of TMS on the surfaces is negligible in the determination of R.

In this work, Ar is used as secondary standard. Intensities of electrons scattered by TMS and Ar at a given angle are recorded at several equilibrium pressures P_s. A typical plot of the scattering intensity I versus $M^{1/2}R$ is shown in Fig. 2 for TMS and Ar at 100 eV and the scattering angle of 25°. It is seen that the measured values for both gases can be very well fitted to a linear function $y = bx$. Following the procedure given in our previous study for e^--tetrahydrofuran collision [22], the ratios between the DCS of TMS and Ar are obtained directly via the ratio between the fitted angular coefficients. Additionally, cross-checking tests of normalization factor were conducted using the equal mean-free-path condition using the hard-spheres diameters of 2.94 and 5.1 Å, respectively, for Ar and TMS, calculated from their van der Waals parameters [23,24]. The obtained DCS have confirmed the validity of the procedure described in Ref. [22]. Absolute DCS for elastic electron scattering on Ar in the 100–1000 eV energy range of Jansen *et al.* [25] are used to normalize our data. The recorded

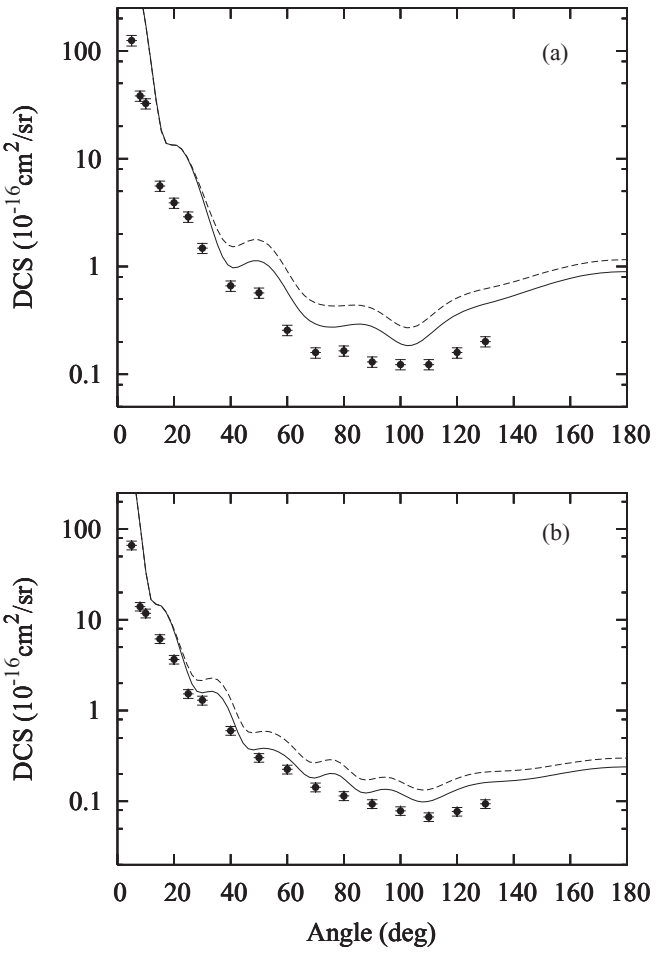

FIG. 3. DCS for elastic e^-–TMS scattering at (a) 100 eV and (b) 200 eV. Full circles, present experimental data; full line, present calculated data using the IAM with absorption; dashed line, present calculated data using the IAM without absorption.

scattering intensities are converted into absolute elastic DCS using the RFT [9,10] according to Eq. (1).

Moreover, the ICS (σ_I) and MTCS (σ_M) are derived from the experimental DCS ($\frac{d\sigma}{d\Omega}$) via numerical integrations:

$$\sigma_I(E) = 2\pi \int_0^\pi \frac{d\sigma}{d\Omega}(E,\theta) \sin\theta d\theta, \tag{3}$$

and

$$\sigma_M(E) = 2\pi \int_0^\pi \frac{d\sigma}{d\Omega}(E,\theta)(1-\cos\theta) \sin\theta d\theta. \tag{4}$$

Details of the analysis of experimental uncertainties have also been given elsewhere [21]. Combining the quoted errors of 6.5% in the absolute DCS of Ar of Jansen *et al.* [25] with all the uncertainties of random and systematic natures associated to the measurements of the scattering intensities and R, we estimate an overall experimental uncertainty of 11% in our absolute DCS. The absolute DCS were determined in the 5°–130° angular range. In order to obtain ICS and MTCS, an extrapolation procedure was adopted to estimate DCS at scattering angles out of the angular range covered experimentally. The extrapolation was carried out manually.

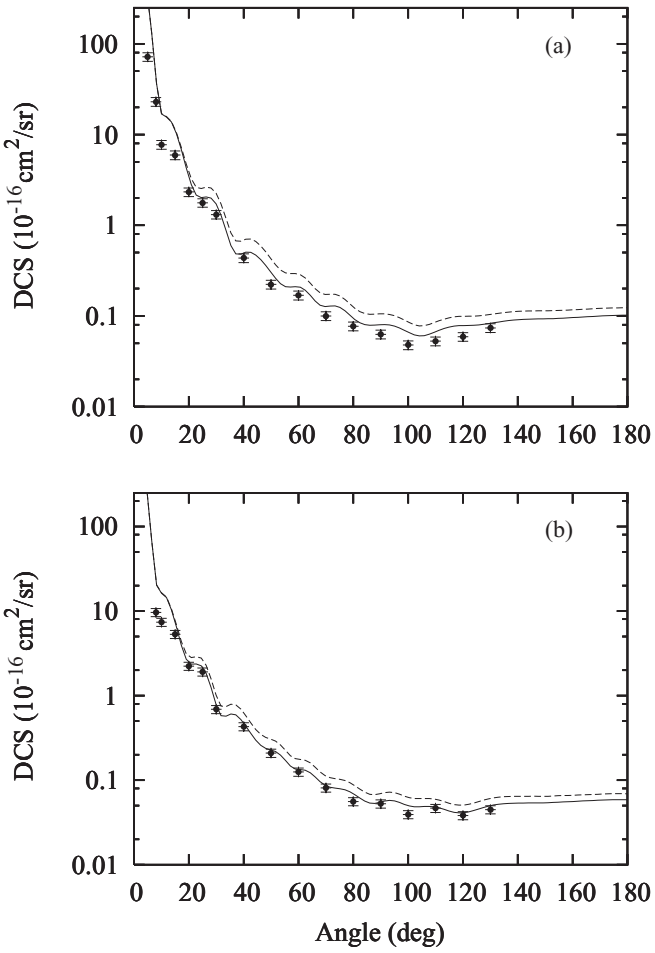

FIG. 4. Same as described in the legend of Fig. 1, but for (a) 300 eV and (b) 400 eV.

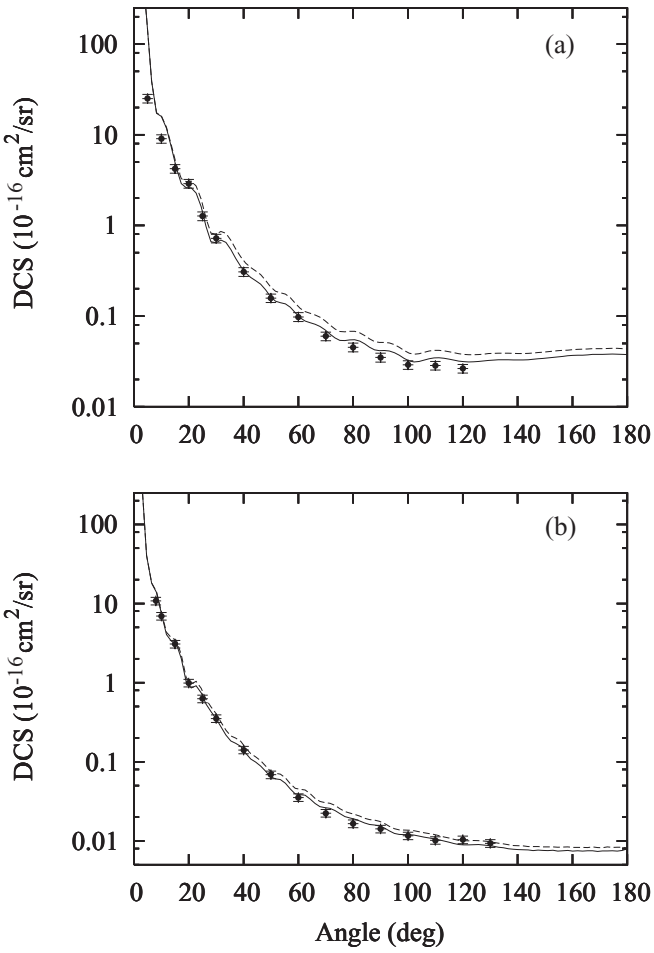

FIG. 5. Same as described in the legend of Fig. 1, but for (a) 500 eV and (b) 1000 eV.

The overall errors on ICS and MTCS are estimated to be 23% in the entire energy range.

III. THEORY

The basic theory of the IAM approach has already been presented in our previous studies [18,22]. For the sake of completeness, it is outlined below. The DCS for elastic electron scattering on a molecule, after averaging over the molecular orientations, is given as

$$\frac{d\sigma}{d\Omega} = \sum_{ij}^{N_{at}} f_i(\theta,k) f_j^*(\theta,k) \frac{\sin(sr_{ij})}{sr_{ij}}, \tag{5}$$

where N_{at} is the number of atoms in the molecule, r_{ij} is the internuclear distance, and $f_i(\theta,k)$ is the scattering amplitude due to the i-th constituent atom. In Eq. (5), $s = 2k\sin(\frac{\theta}{2})$ is the magnitude of the momentum transferred during the collision, and k is the magnitude of the linear momentum of the incident electron. Moreover, atomic scattering amplitudes are obtained by solving the partial-wave radial Schrödinger equation, using the COP to represent the e^--atom interaction. In the present work, the static atomic potentials used are those given by Salvat *et al.* [26]. A model potential proposed by Furness and McCarthy [27] is used to account for the exchange contributions. Moreover, a parameter-free model potential introduced by Padial and Norcross [28] is used to account for the correlation-polarization contributions. The atomic polarizabilities as well as the internuclear distances used in the calculation are taken from the literature [23]. Finally, the absorption contributions were accounted for via version-3 of the quasifree scattering model potential of Staszewska *et al.* [29]. For the generation of exchange, polarization, and absorption contributions, atomic density functions are needed. They are also taken from the article by Salvat *et al.* [26].

The ICS and MTCS for electron-TMS collision are calculated using the additivity rule by summing up, respectively, the ICS and MTCS of all constituent atoms. The ICS of an individual atom is obtained by

$$\sigma_{I,at} = \frac{\pi}{k^2} \sum_{l=0}^{l_{max}} (2l+1)|1 - S_l(k)|^2, \tag{6}$$

where $S_l(k)$ is the scattering matrix element of order l and l_{max} is a truncation parameter. In this work, the value of l_{max} used varies from 80 to 150, depending on the atomic target and also on the energy of the incident electron. In addition, the atomic MTCS are calculated through the numerical integration according to Eq. (4) with the DCS of individual atoms. Also,

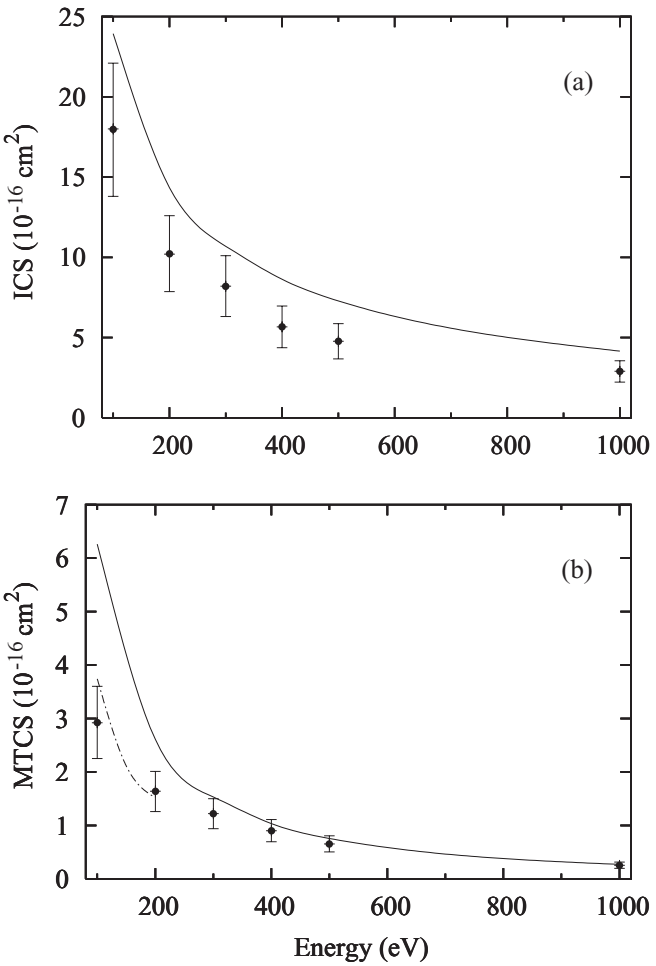

FIG. 6. (a) ICS and (b) MTCS for electron-TMS collisions. Full circles, present experimental data; full line, present calculated data using the IAM-AR with absorption; dashed-dotted line, MTCS of Bordage *et al.* [4] obtained using the swarm analysis technique.

the TCS for electron scattering by the constituent atoms is obtained using the optical theorem:

$$\sigma_{\mathrm{tot},i} = \frac{4\pi}{k} Im[f_i(\theta = 0)]. \quad (7)$$

The TCS for electron-TMS collision is computed using the AR. The difference between the TCS and ICS is the total contribution of the inelastic scattering channels, known as the total absorption cross sections (TACS).

IV. RESULTS AND DISCUSSION

The present experimental data of DCS, ICS, and MTCS, obtained in the 100–1000 eV energy range, are presented in Table I. In Figs. 3–5, we compare our experimental DCS with our results calculated using the IAM at the SEPA level of approximation. For the sake of comparison, IAM data calculated without including the absorption effects are also shown. In general, there is a very good qualitative agreement between the experimental DCS with both theoretical data in the entire energy range studied herein. The oscillations seen in the calculated curves are physical. They can be attributed to the diffraction of the scattering electrons. Since TMS

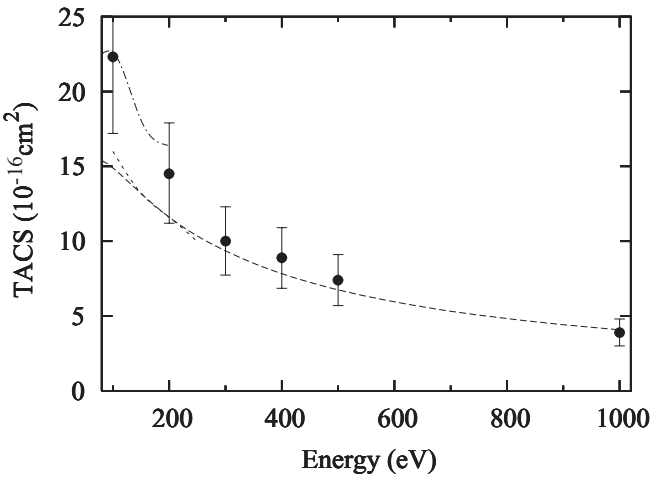

FIG. 7. TACS for electron-TMS collisions. Full circles, present estimated data (see text); dashed-dotted line, TACS of Bordage *et al.* [4] obtained using the swarm analysis technique; dashed line, the BEB TICS [14]; short dashed line, the MAR TICS [13].

is a very symmetrical molecule, the interference between the diffracted outgoing waves are enhanced leading to the appearance of oscillation patterns in the angular distribution of the scattered electrons, which are clearly seen in both the calculated and experimental data. Quantitatively, the IAM calculation at the SEPA level of approximation is in very good agreement with our experiment at incident energies of 300 eV and above. Nevertheless, it overestimates the DCS near the lower-end of incident energies. This discrepancy is expected and has already been observed in other studies [18,22]. Moreover, the comparison between the IAM DCS calculated with and without accounting for the absorption effects show some discrepancies with each other. In general, the IAM DCS calculated in the SEPA approximation are in better agreement with the measured data. It is also seen that the influence of the absorption effects is more relevant at near 100 eV and becomes less important with increasing energy. Therefore, at 1000 eV, a very good quantitative agreement is seen between our experimental DCS with the IAM data calculated both with and without accounting for the absorption effects.

In Fig. 6, we compare our experimental ICS and MTCS for elastic electron scattering by TMS in the 100–1000 eV energy range with the present theoretical data, which were calculated using the AR. The MTCS in the 100–200 eV, derived by Bordage *et al.* [4] using the swarm analysis technique, are also shown for comparison. In the overlapping energy range, our experimental data agree well with those of Bordage *et al.* On the other hand, our IAM-SEPA ICS and MTCS lie systematically above our experimental data. The discrepancy is even larger for ICS than for MTCS. The main reason for this disagreement is due to the fact that in the application of IAM, the polarization effect is taken into account for the individual constituent atoms, which is unphysical. This fact was also discussed in our previous studies [18]. Again, the theory-experiment agreement improves with increasing energies. At some incident energies, marginal agreement is seen.

In Fig. 7, we present our TACS data, which is derived from the difference between the present calculated TCS and measured ICS. The TCS is calculated using the IAM-AR approach. The experimental TACS, which is obtained by summing up the TICS and total excitation cross sections of Bordage *et al.* [4], the calculated TICS of Ali *et al.* [14], and those of Deutsch *et al.* [13], are also shown for comparison. In general, there is a good agreement between our estimated TACS and those derived from swarm technique. Next, although our estimated TACS agree well with both calculated TICS [13,14] in the 300–1000 eV range, they lie above the theoretical TICS at lower energies. This fact is somehow expected, since our TACS account for both the excitation and ionization processes and as it is known, the contribution of ionization is dominant at high energies.

V. CONCLUSION

In summary, in this work, we report an experimental investigation on elastic electron-TMS collisions in the intermediate energy range. The influence of the adsorption of TMS on relative-flow determination is also investigated. Our study shows that the adsorption or desorption on the surfaces inside of the gas-manifold is not important for TMS even at room temperature. On the other hand, our study confirms the important influence of the inelastic scattering channel on the elastic electron-TMS collision, particularly at incident energies near 100 eV. In general, there is a good agreement of our experimental DCS and MTCS with the IAM data calculated at the SEPA level of approximation. Moreover, the TACS derived from the difference of theoretical TCS and experimental ICS also agree fairly well with the existent data derived from swarm analysis technique. The fact that IAM calculation may provide fairly reliable cross sections for electron-TMS collisions at 300 eV and above is very encouraging. Being a very simple method, IAM can be easily applied to investigate electron interaction with larger organometalic compounds for which the experimental studies are, in general, difficult. Further investigation in this direction is desirable.

ACKNOWLEDGMENTS

This research was partially supported by the Brazilian agencies CNPq, CAPES, and FAPESP.

[1] S. Marsden, Beilstein J. Org. Chem. **3**, No. 4 (2007).
[2] P. Kurunczi, A. Koharian, K. Becker, and K. Martus, Contrib. Plasma. Phys. **36**, 723 (1996).
[3] R. Basner, R. Foest, M. Schmidt, F. Sigenerger, P. Kurunczi, K. Becker, and H. Deutsch, Int. J. Mass Spectrom. Ion Proc. **153**, 65 (1996).
[4] M.-C. Bordage, Plasma Sci. Tech. **9**, 756 (2007).
[5] W. Zhang, M. Lelogeais, and M. Ducarroir, Jpn. J. Appl. Phys. **31**, 4053 (1992).
[6] A. Soum-Glaude, G. Rambaud, S. E. Grillo, and L. Thomas, Thin Solid Films **519**, 1266 (2010).
[7] S. McGinnis, K. Riehl, and P. D. Haaland, Chem. Phys. Lett. **232**, 99 (1995).
[8] V. Huber, K. R. Asmis, A.-C. Sergenton, M. Allan, and S. Grimme, J. Phys. Chem. A **102**, 3524 (1998).
[9] S. K. Srivastava, A. Chutjian, and S. Trajmar, J. Chem. Phys. **63**, 2659 (1975).
[10] J. C. Nickel, P. W. Zetner, G. Shen, and S. Trajmar, J. Phys. E **22**, 730 (1989).
[11] M. G. P. Homem, I. Iga, R. T. Sugohara, I. P. Sanches, and M. T. Lee, Rev. Sci. Instrum. **82**, 01319 (2011).
[12] R. T. Sugohara, M. G. P. Homem, I. P. Sanches, A. F. de Moura, M. T. Lee, and I. Iga, Phys. Rev. A **83**, 032708 (2011).
[13] H. Deutsch, K. Becker, R. Basner, M. Schmidt, and T. D. Märk, J. Phys. Chem. A **102**, 8819 (1998).
[14] M. A. Ali, Y.-K. Kim, W. Hwang, N. M. Weinberg, and M. E. Rudd, J. Chem. Phys. **106**, 9612 (1997).
[15] P. Rawat *et al.*, J. Phys. B **43**, 225202 (2010).
[16] G. L. C. de Souza *et al.*, Phys. Rev. A **82**, 012709 (2010).
[17] L. E. Machado, R. T. Sugohara, A. S. dos Santos, M.-T. Lee, I. Iga, G. L. C. de Souza, M. G. P. Homem, S. E. Michelin, and L. M. Brescansin, Phys. Rev. A **84**, 032709 (2011).
[18] I. Iga, I. P. Sanches, E. D. Almeida, R. T. Sugohara, L. Rosani, and M. T. Lee, J. Electron Spectrosc. Rel. Phenom. **155**, 7 (2007).
[19] H. Kato, M. C. Garcia, T. Asahina, M. Hoshino, C. Makochekanwa, H. Tanaka, F. Blanco, and G. Garcia, Phys. Rev. A **79**, 062703 (2009).
[20] I. Iga, M. T. Lee, M. G. P. Homem, L. E. Machado, and L. M. Brescansin, Phys. Rev. A **61**, 227081 (2000).
[21] P. Rawat, I. Iga, M. T. Lee, L. M. Brescansin, M. G. P. Homem, and L. E. Machado, Phys. Rev. A **68**, 052711 (2003).
[22] M. G. P. Homem, R. T. Sugohara, I. P. Sanches, M. T. Lee, and I. Iga, Phys. Rev. A **80**, 032705 (2009).
[23] In *Handbook of Chemistry and Physics*, edited by David R. Lide (CRC Press, Boca Raton, 1992–1993).
[24] C. Yokoyama, T. Takagi, and S. Takahashi, Int. J. Thermophys. **11**, 477 (1990).
[25] R. H. J. Jansen, F. J. de Heer, H. J. Luyken, B. van Wingerden, and H. J. Blaauw, J. Phys. B **9**, 185 (1976).
[26] F. Salvat, J. D. Martinez, R. Mayol, and J. Parellada, Phys. Rev. A **36**, 467 (1987).
[27] J. B. Furness and I. E. McCarthy, J. Phys. B **6**, 2280 (1973).
[28] N. T. Padial and D. W. Norcross, Phys. Rev. A **29**, 1742 (1984).
[29] G. Staszewska, D. W. Schwenke, D. Thirumalai, and D. G. Truhlar, Phys. Rev. A **28**, 2740 (1983).